

Lawrence Berkeley National Laboratory

LBL Publications

Title

Broadband Rotational Spectroscopy in Uniform Supersonic Flows: Chirped Pulse/Uniform Flow for Reaction Dynamics and Low Temperature Kinetics

Permalink

<https://escholarship.org/uc/item/4v51z32c>

Journal

Accounts of Chemical Research, 57(21)

ISSN

0001-4842

Authors

Dias, Nureshan
Suas-David, Nicolas
Thawoos, Shameemah
et al.

Publication Date

2024-11-05

DOI

10.1021/acs.accounts.4c00489

Copyright Information

This work is made available under the terms of a Creative Commons Attribution-NonCommercial License, available at <https://creativecommons.org/licenses/by-nc/4.0/>

Peer reviewed

Broadband Rotational Spectroscopy in Uniform Supersonic Flows: Chirped Pulse/Uniform Flow for Reaction Dynamics and Low Temperature Kinetics

Nureshan Dias, Nicolas Suas-David, Shameemah Thawoos, and Arthur G. Suits*



Cite This: *Acc. Chem. Res.* 2024, 57, 3126–3137



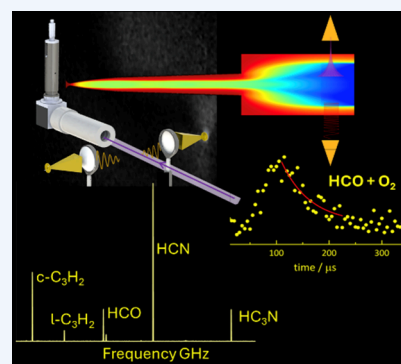
Read Online

ACCESS |

Metrics & More

Article Recommendations

CONSPECTUS: The study of gas-phase chemical reactions at very low temperatures first became possible with the development and implementation of the CRESU (French acronym for Reaction Kinetics in Uniform Supersonic Flows) technique. CRESU relies on a uniform supersonic flow produced by expansion of a gas through a Laval (convergent-divergent) nozzle to produce a wall-less reactor at temperatures from 10 to 200 K and densities of 10^{16} – 10^{18} cm^{-3} for the study of low temperature kinetics, with particular application to astrochemistry. In recent years, we have combined uniform flows with revolutionary advances in broadband rotational spectroscopy to yield an instrument that affords near-universal detection for novel applications in photodissociation, reaction dynamics, and kinetics. This combination of uniform supersonic flows with chirped-pulse Fourier-transform microwave spectroscopy (Chirped-Pulse/Uniform Flow, CPUF) permits detection of any species with a modest dipole moment, thermalized to the uniform temperature of the gas flow, with isomer, conformer, and vibrational state specificity. In addition, the use of broadband, high-resolution, and time-dependent (microsecond time scale) micro- and mm-wave spectroscopy makes it an ideal tool for characterizing both transient and stable molecules, as well as studying their spectroscopy and dynamics.



In this Account, we review recent advances made using the CPUF technique, including studies of photodissociation, radical–radical reaction dynamics, and low temperature kinetics. These studies highlight both the strength of universal and multiplexed detection and the challenges of coupling it to a high-density collisional environment. Product branching and product evolution as a function of time have been measured for astrochemically relevant systems, relying on the detailed characterization of these flow conditions via experiments and fluid dynamics simulations. In the photodissociation of isoxazole, an unusual heterocyclic molecule with a very low-energy conical intersection, we have identified 7 products in 5 reaction channels and determined the product branching, pointing to both direct and indirect pathways. We have also approached the same system from separated NO and C_3H_3 reactants to explore a broader range of the potential energy surface, demonstrating the power of multichannel branching measurements for complex radical–radical reactions. We determined the product branching in the C_3H_2 isomers in the photodissociation of the propargyl radical and identified the importance of a hydrogen atom catalyzed isomerization to the lowest energy cyclic form. This then motivated a study of direct D-H exchange reaction in radicals, in which we demonstrate that it is an important and overlooked pathway for deuterium fractionation in astrochemical environments. Recently, we have shown the measurement of low temperature kinetics inside an extended Laval nozzle, after which a shock-free secondary expansion to low temperature and density affords an ideal environment for detection by rotational spectroscopy. These results highlight the power and potential of the CPUF approach, and future prospects will also be discussed in light of these developments.

KEY REFERENCES

- Oldham, J. M.; Abeysekera, C.; Joalland, B.; Zack, L. N.; Prozument, K.; Sims, I.; Park, G. B.; Field, R. W.; Suits, A. G. A chirped-pulse Fourier-transform microwave/pulsed uniform flow spectrometer. I. The low-temperature flow system *J. Chem. Phys.* **2014** *141*, 154202.¹ This paper introduces the concept of combining a uniform supersonic flow with chirped-pulse rotational spectroscopy. The novel pulsed flow system is described in detail.
- Broderick, B. M.; Suas-David, N.; Dias, N.; Suits, A. G. Isomer-specific Detection in the UV Photodissociation of the Propargyl Radical by Chirped-Pulse mm-Wave

Received: July 27, 2024
 Revised: September 23, 2024
 Accepted: September 24, 2024
 Published: October 15, 2024



Spectroscopy in a Pulsed Quasi-Uniform Flow. *Phys. Chem. Chem. Phys.* **2018**, *20*, 5517–5529.² *The quasi-uniform flow is introduced and applied to show the time dependence of C₃H₂ isomer formation in propargyl radical dissociation. H atom catalyzed isomerization in the flow is shown to transform the linear into the most stable cyclic isomer.*

- Dias, N.; Gurusinghe, R. M.; Suits, A. G. Multichannel Radical–Radical Reaction Dynamics Probed by Broadband Rotational Spectroscopy: Propargyl + NO *J. Phys. Chem. A* **2022**, *126*, 5354–5362.³ *The reaction is shown to give HCN, HNC, HCNO, CH₂CN, CH₃CN, HC₃N, CH₂CO and HCO, while spectral intensities of pure-rotational lines allow product branching to be quantified. Theoretical calculations show the product branching depends significantly on the initial excitation in the radical precursor.*
- Thawoos, S.; Suas-David, N.; Gurusinghe, R. M.; Edlin, M.; Behzadfar, A.; Lang, J.; Suits, A. G. Low temperature reaction kinetics inside an extended Laval nozzle: REMPI characterization and detection by broadband rotational spectroscopy. *J. Chem. Phys.* (2023) *159*, 214201.⁴ *Reaction kinetics are measured inside an extended Laval nozzle, and the conditions there and in a secondary expansion are monitored by resonant photoionization. This yields a general approach to perform low temperature kinetics while still achieving optimal conditions for detection by rotational spectroscopy.*

1. INTRODUCTION

Surprising chemical complexity is seen in the large inventory of molecules now detected in interstellar and circumstellar environments, and the widely varying conditions of density, temperature, and radiation load in these sources make it a challenge to unravel the mechanisms that form these molecules.⁵ To understand the chemistry in these remote environments, experimentalists replicate the conditions in the laboratory and simply make measurements. However, the densities are many orders of magnitude lower than the lowest pressures accessible in the laboratory, collision frequencies typically measured in terms of years rather than nanoseconds and mean free paths of hundreds of kilometers. As a result, it is necessary to develop experiments which can be applied to understand select key aspects underlying the formation or destruction of molecules in space rather than attempting to replicate the conditions exactly.⁶

One of the most important such methods has been the CRESU technique (a French acronym meaning “reaction kinetics in uniform supersonic flows”) developed by Rowe and co-workers.⁷ This method relies on supersonic expansion of a gas via a Laval nozzle, a convergent-divergent nozzle familiar as the shape of a rocket-nozzle. If the upstream and downstream pressures are controlled to match the nozzle’s design parameters, the result is a collimated, low-temperature gas flow. Unlike a typical molecular beam, however, this is a collisional environment at a uniform temperature and density, and it may be centimeters in diameter with densities typically over 10^{16} cm⁻³. This provides a wall-less reactor in which the kinetics of astrochemically relevant reactions have been studied down to 6 K.⁸ When the method was first developed in the 1980s, it was believed that only ion–molecule reactions lacking any activation energy could make a significant contribution to

the chemistry in cold astrophysical environments. CRESU experiments showed, however, that many radical–molecule reactions may be barrierless, thus remaining very fast at low temperature, and can play an important role in molecular growth and transformation even in cold, dark molecular clouds at 10–50 K and densities 10^4 – 10^6 cm⁻³.^{9,10}

The CRESU method has since been implemented in many laboratories around the world, and most of them use laser-induced fluorescence (LIF) as the method of detection.¹¹ LIF has the advantage that it is extremely sensitive and can readily be employed in Laval flows where the collision frequency may be up to 10 MHz. It has some disadvantages, however: the most significant is the limited number of systems that are available for LIF detection. LIF is most favorable for systems with convenient, long-lived excited electronic states that exhibit strong fluorescence, readily accessed with tunable dye lasers in the visible or near-UV. Important examples include CN,^{9,12–15} OH,^{10,16–18} and CH.^{19–22} Some atomic species have also recently been probed in CRESU experiments using vacuum ultraviolet (VUV) LIF,^{23,24} but this is quite challenging. Another limitation of LIF detection is that it cannot readily be used in multiplexed approaches or for determining product branching. Nevertheless, it has proven to be extremely important in measuring reaction kinetics for many astrochemical and atmospheric reactions. One alternative probe technique, first developed by Leone at the Advanced Light Source, is VUV photoionization mass spectrometry,²⁵ also used more recently by the Rennes group at the SOLEIL synchrotron.²⁶ This is a sensitive and universal detection method but requires a low density in the probe region to prevent interference from ion–molecule reactions that might occur en route to detection. To address this challenge, the flow is sampled using a skimmer or airfoil with a small aperture. Although the sampling strategy can be effective, questions remain about shocks at the entrance to the sampling orifice or just after it that may alter the conditions. These issues will be considered in greater detail below.

In 2008, the Pate group at the University of Virginia reported a novel approach to rotational spectroscopy that delivered a thousand-fold (or more) increase in the data acquisition rate or “spectral velocity” compared to the traditional cavity-based Balle-Flygare approach.²⁷ This method, Chirped-pulse Fourier-Transform Microwave (CP-FTMW) Spectroscopy, takes advantage of modern high-speed electronics to produce a high-power frequency sweep of several GHz in a microsecond or less that irradiates the sample. The free induction decay (FID) of the coherently excited sample is averaged in the time domain, and then, after down-conversion and Fourier transform, any molecules excited are detected with fingerprint signatures and reliable abundances. Not long after this development, we recognized that the low-temperature uniform flow environment would be ideal for application of the CP-FTMW method, as reaction products could be cooled in the flow to reduce the rotational partition function, a necessary step to achieve sensitive detection by rotational spectroscopy.^{1,28} The approach, termed Chirped Pulse/Uniform Flow (CPUF), could then be used to study product branching in photodissociation or bimolecular reactions and applied to low temperature kinetics as well. We note Sims et al. recently developed a CPUF apparatus for continuous uniform flows, and they have shown both reaction²⁹ and line width measurements³⁰ directly in the flow.

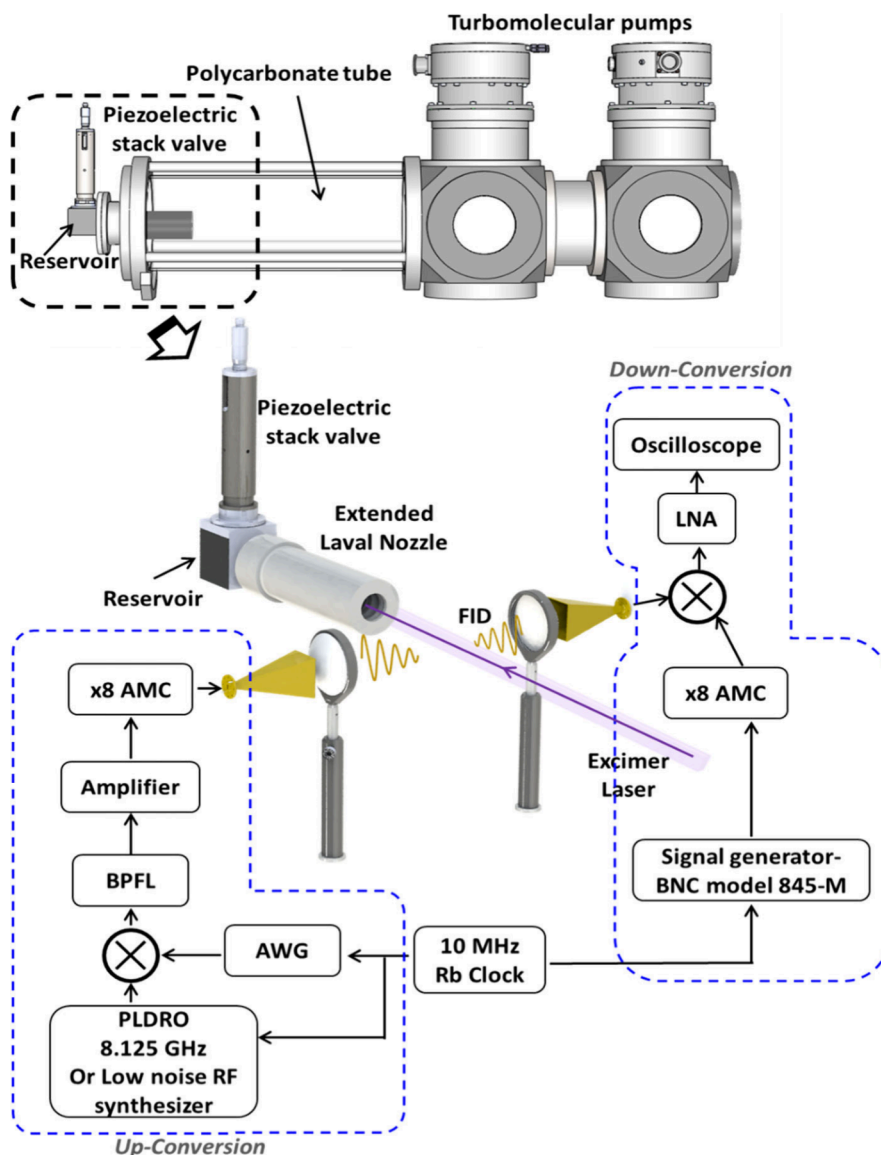


Figure 1. Schematic representation of the CPUF instrumentation. Linearly chirped pulses (0.25–3.75 GHz) are produced in an arbitrary waveform generator (AWG) and then mixed with a PLDRO (frequency 8.125 GHz) or a BNC RF synthesizer locked to a 10 MHz Rb standard. The resulting frequencies are then multiplied, amplified, and broadcast onto the flow via a feedhorn that is oriented perpendicular to the flow axis. Bandpass filters and isolators are inserted into the setup as necessary. The pulsed uniform flow source consists of a piezoelectric stack valve,³⁷ connected to mass flow controllers (MFCs), and a Laval nozzle mounted on one end of a polycarbonate vacuum chamber.¹ A quartz window is located on the other end of the chamber to allow radiation from an ArF excimer laser to propagate down the axis of the Laval nozzle such that the core of the flow is irradiated. The resultant molecular emission from the core is collected as free induction decay (FID) by a second feedhorn, amplified through a low noise amplifier (LNA), down-converted before detection, and phase-coherently averaged in an oscilloscope, where it is fast Fourier-transformed to produce a frequency-domain spectrum.

In this Account, we describe this approach, termed Chirped Pulse/Uniform Flow (CPUF), and illustrate both the strengths of the method and the challenges that must be overcome to optimize its performance. In Section 2, we present the experimental method, describing both our implementation of a pulsed uniform supersonic flow and the CP-FTMW spectrometer. We also introduce the “quasi-uniform flow” and the computational fluid dynamics (CFD) investigations we have used to understand the flow performance throughout this work.² We then turn to applications, showing in two cases how CPUF studies of multichannel branching in photodissociation can complement and enrich related studies of bimolecular reactions. In Section 3, we show how our studies of propargyl radical photodissociation² led to the identification of D-H

exchange in radicals as an overlooked pathway to interstellar deuterium enrichment.³¹ Section 4 presents two distinct approaches to exploring the C_3H_3NO potential surface: one by photodissociation of isoxazole³² and another by the $C_3H_3 + NO$ reaction.³ Application of CPUF to kinetics is described in Section 5, achieved by performing the reaction entirely *inside* an extended nozzle.⁴ Finally, we point to future opportunities and challenges for the CPUF method.

2. THE EXPERIMENTAL APPROACH

Here, we introduce the CPUF instrument, shown in Figure 1, and highlight some unique features both in the Laval flow system and in the spectrometer. In generating the uniform flow, we made some design choices that diverge from those

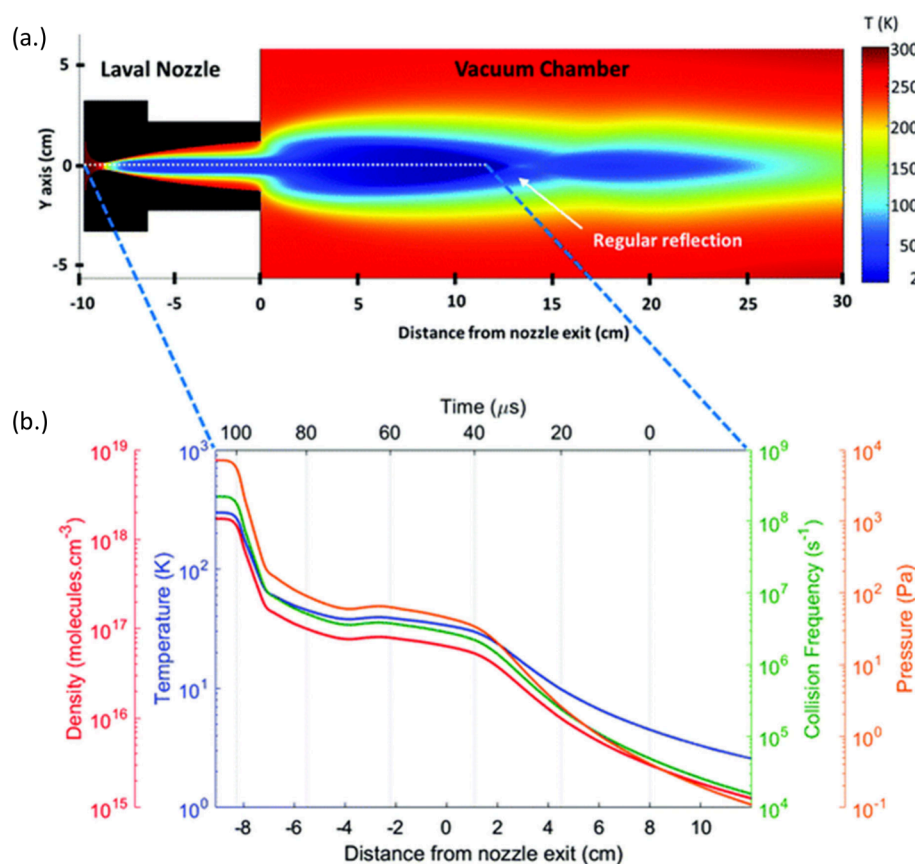


Figure 2. (a) Distribution of the temperature calculated from CFD simulations. (b) Evolution of various thermodynamic properties (temperature, density, pressure, and collision frequency) along the axis of the flow from the reservoir to the shock layer in the vacuum chamber. Reproduced with permission from ref 2. Copyright 2018 The Royal Society of Chemistry.

generally employed elsewhere.¹ First, we chose to use a pulsed flow as originally developed by Atkinson and Smith³³ and widely used in CRESU implementations outside of Rennes.^{18,34–36} However, rather than using solenoid valves, we developed a high-throughput pulsed valve based on a stacked piezo actuator.³⁷ This allows us to fill a 15 cm³ reservoir to the target pressure despite the large throat aperture (3–10 mm) of the Laval nozzle, ensuring high quality pulsed flows at low temperature. In addition, we employ a high-throughput magnetically suspended turbomolecular pump (in fact, two of these in the present apparatus). Another distinct feature of the apparatus is the chamber itself, which is a large polycarbonate tube through which we send microwave excitation and detect the FID from the excited molecules. The goal here is to minimize the reflections off of metal surfaces that can interfere with the recorded signals.

The CP-FTMW approach relies upon a high bandwidth (8 GS/s) arbitrary waveform generator to produce a linear frequency sweep (or perhaps a series of single-frequency bursts) that is amplified and mixed with a fixed frequency produced by a PLDRO or an RF synthesizer and frequency-multiplied to the region of interest before being broadcast into the sample. The emitted FID is down-converted and averaged in the time domain in a high-bandwidth oscilloscope (4 GHz analog bandwidth). The spectrometer we developed initially operated in the Ka band from 26 to 40 GHz and relied upon a 40 W traveling wave tube amplifier to excite the sample.²⁸ We subsequently changed to the mmWave regime, 60–92 GHz, and all the data presented here was obtained using variations of

this spectrometer configuration which is based on that of Park et al. (Figure 1).³⁸ Although the available power in the mmWave regime is 3–4 orders of magnitude lower, the fact that the signal scales as the square root of the power, the focal volume is much smaller, and the 20 K Boltzmann population for 3–6 heavy atom molecules peaks closer to this spectrometer window means only a modest price is paid in signal for the greater versatility of the mmWave regime and the access to smaller molecules such as HCO and HCN.

Rotational spectroscopy is a near-universal technique in that almost any molecule with a dipole moment can be detected. In general, it is less sensitive than LIF or photoionization. The signal depends quadratically on the dipole moment and scales linearly with the inverse of the rotational partition function. The results shown here highlight the range of molecules that can readily be detected.

Although ideally one would wish to probe the reaction directly in the flow, the collision frequency is typically too high to permit this as collisions interfere with the creation of the coherent excitation as well as the FID. Instead, we have developed an alternative strategy in which the chamber pressure is reduced well below the design target for the nozzle, giving a “quasi-uniform flow” that is uniform within the nozzle (or nearly so) but undergoes a second expansion to low density and temperature which is ideal for detection by CP-FTMW. We have implemented this in our 20 K high density (2×10^{17} molecules cm⁻³) helium nozzle.² This approach allows time for reactions to take place and for cooling of the reaction products while still giving excellent sensitivity in the

probe region. We used CFD modeling of the flow to understand its properties and to aid in interpreting the results. The simulation results are shown in Figure 2. Figure 2(a) shows the overall 2D temperature profile from the nozzle throat to the chamber itself. The mmWave probe is located 8 cm from the exit of the nozzle. Figure 2(b) shows the evolution of key thermodynamic parameters along the axis of the flow. The lower abscissa scale in Figure 2(b) shows the distance from the nozzle exit, while the upper scale gives the corresponding “birth time” relative to the probe time based on the flow velocity. This highlights this very useful feature of the flow that the spatial origin is mapped to arrival time. The figure shows the steep density drop that accompanies the initial expansion from the nozzle throat from 100 to 90 μs before detection, which is followed by a temperature near 40 K for the next 50 μs or so. The high collision frequency here promotes rapid rotational thermalization to the flow temperature and slower vibrational relaxation that is sometimes observed. After the nozzle exit, there is a second expansion that leads to temperatures around 5 K and collision frequencies at 100 kHz or below for detection by CP-FTMW. This quasi-uniform flow is suitable for studying photochemistry and bimolecular reactions focused on product branching but is less so for kinetic measurements in which temperature and density must be carefully controlled for the duration of the measurement. For kinetics applications, we expand on the idea of the secondary expansion by extending the nozzle length and performing the kinetics *inside* the nozzle itself.⁴ The secondary expansion again gives conditions optimized for detection. This is described in detail in Section 5 below.

3. PROPARGYL PHOTODISSOCIATION AND D-H EXCHANGE IN RADICALS

In this section, we show how insights obtained studying propargyl radical photodissociation in the flow environment led to a study of bimolecular chemistry with significant astrochemical implications. Propargyl radical, CH_2CCH , is a ubiquitous resonance-stabilized radical found in combustion environments^{39,40} and recently detected in the Taurus Molecular Cloud (TMC-1) in great abundance.⁴¹ It is challenging to detect by rotational spectroscopy owing to its small dipole moment (0.15 D), but it is known to be a central player in hydrocarbon combustion and in models of Titan’s atmosphere as well.⁴² In our CPUF study, either propargyl bromide or 1,2-butadiene, was used as a photolytic precursor for the formation of the propargyl radical. Absorption of a second photon then can lead to photodissociation of the radical and formation of hydrogen atom and a range of C_3H_2 radicals as the primary pathway.^{43,44} These radical products include both linear $\text{l-C}_3\text{H}_2$ and cyclic $\text{c-C}_3\text{H}_2$ and triplet propargylene, HCCCH. The first two are readily detected by rotational spectroscopy: $\text{c-C}_3\text{H}_2$ was the first cyclic species to be detected in space, and both are seen in a wide variety of sources.⁴⁵ Propargylene, however, has a negligible dipole moment and is undetectable by rotational spectroscopy. Nevertheless, we were able to infer its presence and quantify it, as described below.

In this experiment, 1% 1,2 butadiene is seeded in the helium quasi-uniform flow and dissociated at 193 nm. The products are detected using a burst of single frequency $\pi/2$ pulses (i.e., with the duration chosen to maximize the coherence for each target species), followed by a listening time of several microseconds during which the FID is recorded. This is

repeated at 10 μs intervals following laser photolysis to trace the chemistry occurring in the flow. The overall repetition rate of the experiment is 5–10 Hz. The results are shown in Figure 3. Here and elsewhere, the transitions are labeled as J_{KaKc} for

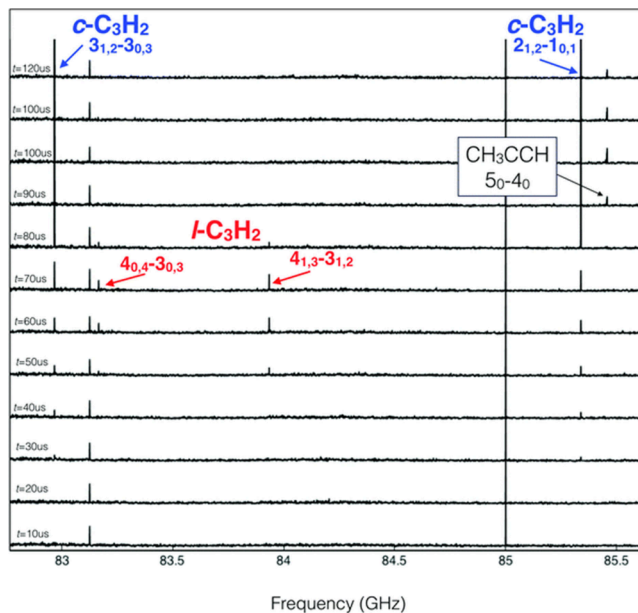


Figure 3. Microwave spectra of photoproducts arising from the 193 nm photodissociation of the propargyl radical. Four single-frequency $\pi/2$ pulses corresponding to the $3_{1,2}-3_{0,3}$ (82.966 GHz) and $2_{1,2}-1_{0,1}$ (85.338 GHz) transitions of $\text{c-C}_3\text{H}_2$, and $4_{0,4}-3_{0,3}$ (83.165 GHz) and $4_{1,3}-3_{1,2}$ (83.933 GHz) transitions of $\text{l-C}_3\text{H}_2$ irradiate the sample. A fifth line due to the 5_0-4_0 transition of propyne is observed nearby at 85.457 GHz excited off-resonance. The times are offset 20 μs relative to those in Figure 2. Reproduced with permission from ref 2. Copyright 2018 The Royal Society of Chemistry.

asymmetric tops and J_K for symmetric top molecules. The cyclic radical is seen promptly, 30 μs after the laser fires, with the weaker signal from the linear isomer appearing somewhat later. The remarkable aspect of the results is the distinct subsequent behavior of the signals: The $\text{l-C}_3\text{H}_2$ signal decays at 70–80 μs just as the $\text{c-C}_3\text{H}_2$ signal grows dramatically up to 20 times larger than its onset. This is understood to be the result of H atom catalyzed isomerization: recombination of C_3H_2 radicals with H atoms that are also produced in the dissociation of the precursor will produce propargyl radicals that will again decompose, but given the low energy available following the recombination in the cold flow, they exclusively produce the lowest energy species, $\text{c-C}_3\text{H}_2$. The much larger growth seen at the later times is attributed to the same process occurring for the propargylene species: this allows us to estimate the branching for that product as well. The results are summarized in Table 1 and compared to calculations from Nguyen et al.⁴⁴ Reasonable agreement is found, except that the CPUF results suggest a larger branching to the cyclic species. The discrepancy was attributed to a higher barrier (and asymptotic energy) for decomposition to $\text{c-C}_3\text{H}_2$ than subsequently found in very high-level calculations.⁴⁵ Note that the spectra also show the appearance of propyne very late in the flow corresponding to the high-density region at the throat of the nozzle. This is the result of recombination of the propargyl radical with H atoms that are then stabilized by third-body collisions. Allene formation is also possible by the

Table 1. Experimental Branching Fractions (%) in Comparison with Those Computed by Nguyen et al. in the 193 nm Photodissociation of the Propargyl Radical from Ref 44^a

	c-C ₃ H ₂ + H	l-C ₃ H ₂ + H	³ HCCCH + H	C ₃ H + H ₂
This work	16.8 ^(+3.2/-1.3)	2.9 ^(+1.1/-0.5)	80.2 ^(+1.8/-4.2)	0 ⁽⁺¹⁾
Nguyen et al. ⁴⁴	3.60	3.50	86.50	5.50

^aAlthough we did not directly detect C₃H, we place an upper bound of 1% branching to this channel on the basis of the noise floor in the spectrum at the location of its 3-2 transition at 80388.1 MHz.

same mechanism but cannot be detected by rotational spectroscopy.

These results then suggested that a similar reaction involving D atoms, at the low temperature of the flow or in cold interstellar clouds, should produce c-C₃HD by an analogous mechanism. The exothermicity of the process c-C₃H₂ + D → c-C₃HD + H is 7.5 kJ mol⁻¹, and of course larger for D-H exchange in the other C₃H₂ isomers, to give c-C₃HD.³¹ Similar considerations apply for the transformation of C₃H₃ to C₃H₂D and C₃H₄ isomers to their deuterated isotopologues. We thus performed an analogous experiment except in this case we added ND₃ as a source of D atoms, and the results are shown in Figure 4. We indeed see formation of c-C₃HD as anticipated, but no evidence for doubly deuterated species nor of l-C₃HD. We also see both forms of deuterated propyne. These may be formed by D-H exchange in the propargyl radical followed by H addition and stabilization or by D addition and stabilization to normal propargyl radicals. We found that the relative yield of these was sensitive to experimental conditions suggesting complex and competing pathways.

Motivated by these findings, we performed modeling of two interstellar cloud conditions in collaboration with T. J. Millar at Queen's University, adding these D-H exchange reactions that

had not previously been included. The models showed a significant impact on the abundance and deuterium fractionation for both a TMC-1 type cloud and a warmer Orion Ridge Cloud condition. We found that, under cold conditions of TMC-1, more than 78% of the c-C₃HD is formed by the D-H exchange mechanism, while in warmer conditions it is 69%. The results suggest the importance of including D-H exchange involving radicals in a more comprehensive model and one that can explicitly include nuclear spin effects which were absent in our preliminary study.

4. ISOXAZOLE PHOTODISSOCIATION AND THE NO + C₃H₃ REACTION

We now turn to an examination of chemistry on the C₃H₃NO potential energy surface, approaching it from two distinct starting points: photodissociation of the isoxazole molecule, c-C₃H₃NO, and from the NO + C₃H₃ bimolecular reaction. Key stationary points on the potential surface are shown in Figure S, synthesized from calculations reported in refs 46 and 47. The isoxazole molecule is shown as IM5 in Figure 5.

The crossing between the ππ* and πσ* excited potential surfaces in heterocyclic aromatic molecules such as pyrrole and furan has been found to control the dissociation dynamics, leading to many studies of the dynamics at this conical intersection (CI) in these and related molecules.⁴⁸ Although it is isoelectronic with furan and pyrrole, isoxazole exhibits quite distinct excitation and decay dynamics owing to ring opening via a low-lying CI involving a singlet biradical β-formyl vinyl nitrene intermediate (TS10). Isoxazole dissociation has been studied using surface hopping dynamics calculations,⁴⁹ by pyrolysis with IR probing of the intermediates and products and extensive electronic structure calculations⁵⁰ and more recently by time-resolved photoelectron spectroscopy.⁵¹ Based on previous studies, we infer that the dissociation of isoxazole can be characterized as an ultrafast process where N–O bond cleavage immediately occurs and is followed by internal

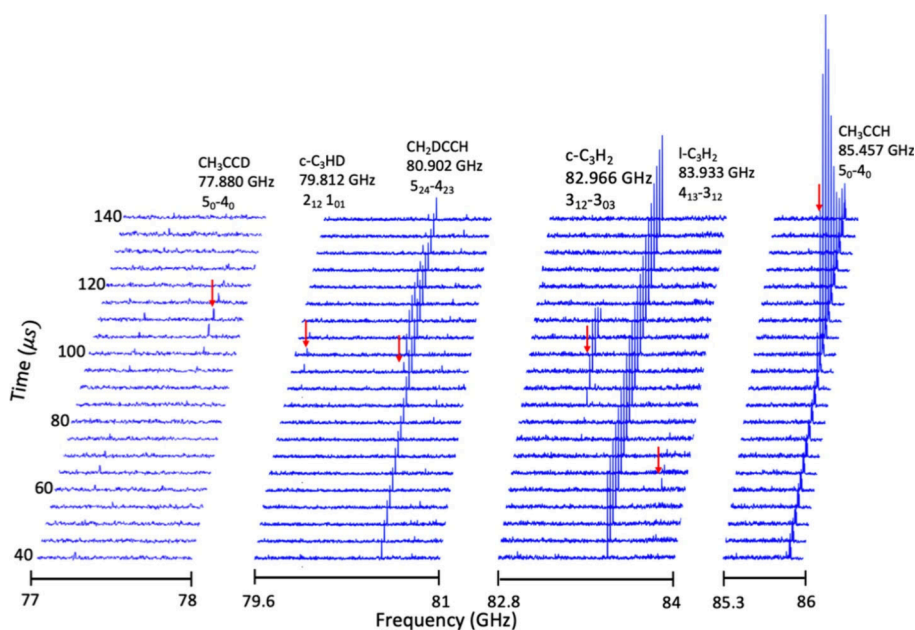


Figure 4. Rotational spectra of the products observed in the 193 nm dissociation of propargyl bromide and ND₃. Probe delay after laser pulse is indicated on the left. The red arrows indicate the positions of each rotational line observed, and the details of each line are indicated just above it. The times are offset 20 μs relative to those in Figure 2. By N. Dias et al. Reproduced from ref 31, 2022. Licensed under CC-BY 4.0.

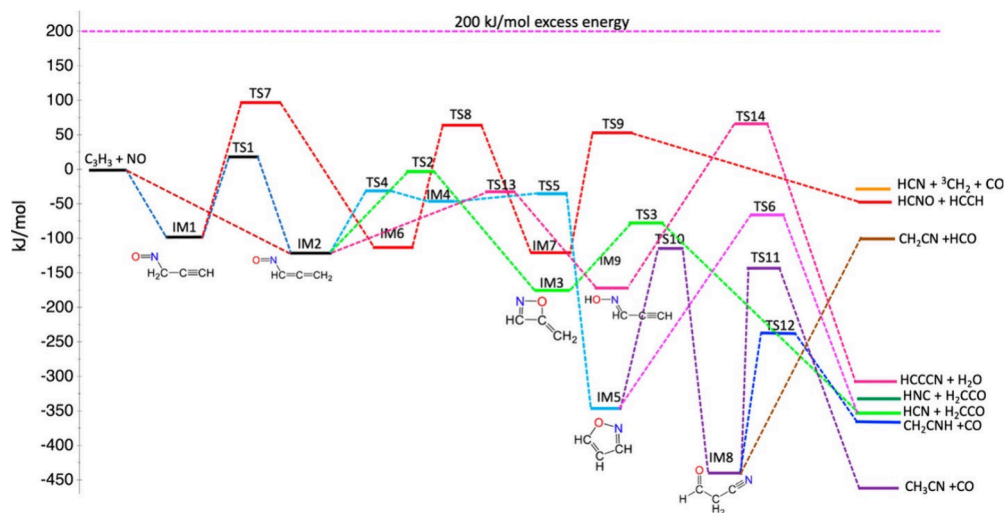


Figure 5. Key stationary points on the potential energy surface for the NO + C₃H₃ reaction. The energetics and pathways are based on high-level theoretical calculations by Wang et al. and Danilack and Goldsmith from refs 46 and 47, respectively. Reproduced from ref 3. Copyright 2022 American Chemical Society.

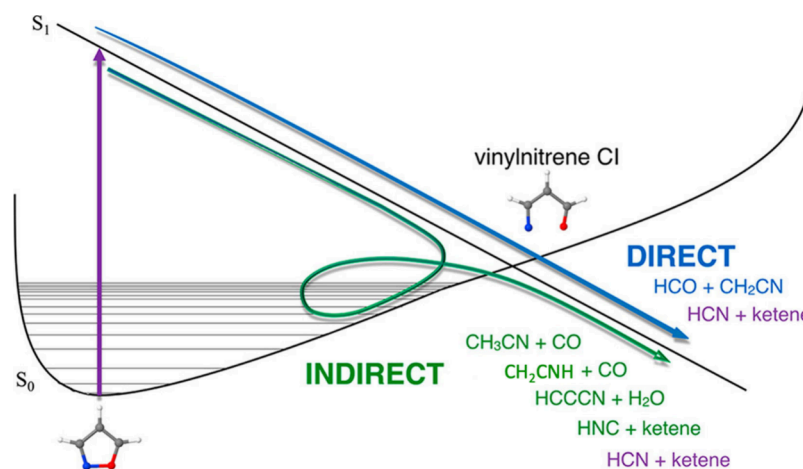


Figure 6. Qualitative illustration of the decomposition pathways of isoxazole. Reproduced from ref 32. Copyright 2018 American Chemical Society.

conversion to the ground state at the low-lying conical intersection. This internal conversion leads either directly to certain products by ultrafast dissociation or to a more protracted exploration of the ground state ultimately yielding other products consistent with thermal decomposition. Both direct and indirect dissociation occur through this CI. This discrimination between direct and indirect pathways was based on a comparison of the product yields to those from the pyrolysis experiments and the ultrafast surface hopping dynamical calculations. The primary decomposition pathway observed for isoxazole dissociation yields HCN and CH₂CO (³CH₂ + CO), representing a predominantly nonstatistical, ultrafast, direct process immediately following internal conversion to S₀. Similarly, HCN, HCO, and CH₂CN are produced directly. Additionally, we confirm that the products CH₃CN, HCCCN, and HNC are produced via an indirect mechanism extensively involving dynamics in the ground state. The qualitative illustration of the decomposition pathways of isoxazole is shown in Figure 6.

We subsequently approached the isoxazole system from a bimolecular radical–radical reaction of NO with C₃H₃. In these experiments, the propargyl radical is formed from the

193 nm photodissociation of either 1,2-butadiene (see section 3) or propargyl bromide (0.5% C₃H₃Br or CH₂CCHCH₃ with 0.5% NO, seeded in He). Broad scans were used to identify the reaction products, and then, $\pi/2$ pulses were used to maximize the signals. The comparison of product branching fractions obtained for both studies is shown in Table 2. As shown in Figure 5, isoxazole is an important minimum on the PES of the reaction of C₃H₃ with NO. Many bimolecular products are

Table 2. Product Branching (%) Observed for the NO + C₃H₃ Compared with Isoxazole Photodissociation

species	branching branching	
	NO + C ₃ H ₃	isoxazole dissociation
HCN	50.5 (+6.4/−4.0)	53.8 (±1.7)
HCNO	18.9 (+1.8/−0.8)	
CH ₂ CN	11.7 (+0.8/−0.3)	7.8 (±2.9)
CH ₃ CN	7.4 (+1.2/−0.7)	23.4 (±6.8)
HC ₃ N	6.2 (+2.6/−2.1)	0.9 (±0.2)
HNC	2.3 (+0.3/−0.2)	0.9 (±0.2)
CH ₂ CO	1.3 (+0.5/−0.4)	3.8 (±0.9)
HCO	1.8 (+0.2/−0.1)	9.5 (±2.3)

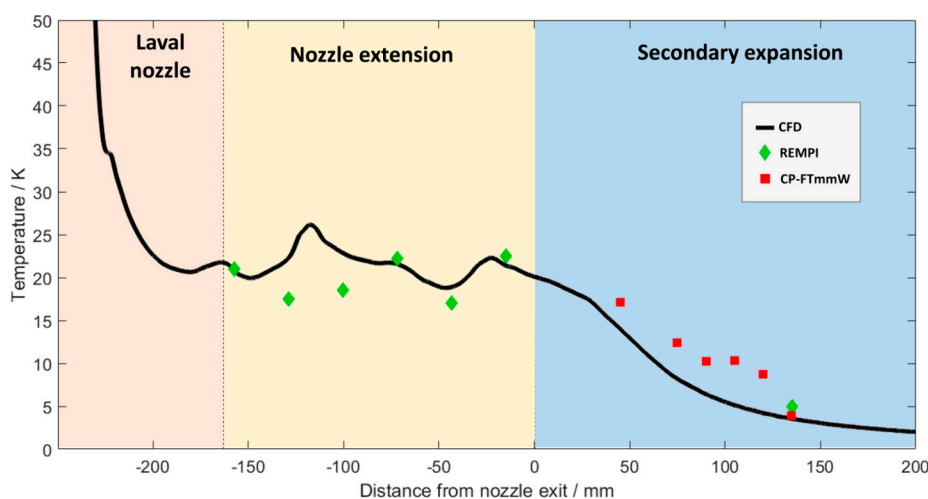


Figure 7. Comparison of theoretical and experimental temperatures of the flow along the axis of the extended nozzle along with the secondary expansion. Solid black line is the CFD simulation of the temperature. Green diamonds are the temperature of the flow retrieved by REMPI spectra of the dilute sample of NO, and red squares represent the temperature of the secondary expansion obtained by the CP-FT mmW spectra of furan. Reproduced with permission from reference 4. Copyright 2023, AIP.

formed from isoxazole through the key intermediate β -formylvinylnitrene. Just as in isoxazole photodissociation, HCN was observed as a major product, and the branching fractions are comparable. However, in both cases, the coproduct CH_2CO is nonstoichiometric with HCN. From these two experiments, we confirm that the coproduct CH_2CO undergoes secondary dissociation to form triplet methylene and CO. Triplet methylene readily reacts with NO to produce HCNO, and the reaction is fast and barrierless. HCNO emerges as the second most abundant product observed in the $\text{NO} + \text{C}_3\text{H}_3$ reaction but is thus not a primary product. We find that the combined branching of HCNO and CH_2CO is comparable to the branching of HCN. The absence of NO in the isoxazole study accounts for the absence of HCNO in that case. The third most abundant channel we observed in the $\text{NO} + \text{C}_3\text{H}_3$ reaction was $\text{CH}_2\text{CN} + \text{HCO}$. We observed lower branching for HCO, and we attribute this to secondary decomposition or reaction of this radical, given its weak (~ 18 kcal/mol) C–H bond energy. This work also highlighted the importance of the excess energy possessed by the photolytically prepared reactant molecules as energy barriers can be overcome. We found this excess energy was critical to the formation of HCCCN and HNC. The pathway leading to HCCCN requires 69 kJ/mol of energy (TS14), while the reactant molecules possess approximately 200 kJ/mol of energy, which is sufficient to overcome that barrier. Similarly, there is a possibility of isomerization of hot HCN to HNC. The isomerization of HCN to HNC proceeds via highly excited bending states and a barrier of 187 kJ/mol.⁵² At the energy of the reaction, it is likely that both HNC and HCN are formed and a fraction is quenched to the HNC side of the barrier.

In addition to ground state molecules, we detected two vibrationally excited HCN states in the $\text{NO} + \text{C}_3\text{H}_3$ reaction. These excited molecules appear earlier in the flow than the ground vibrational state HCN products, suggesting vibrational cooling in the high-density region at the nozzle throat. Typically, vibrational cooling is considerably less efficient than rotational cooling, but due to the possibility of upward of 10^4 collisions with helium, it may still occur.

5. LOW TEMPERATURE KINETICS

Next, we explore CPUF applications in reaction kinetics. The use of microwave detection for kinetics was pioneered by Koda et al. for studies at room temperature.⁵³ This is challenging given the temperature scaling of the rotational partition function, and this is one of the motivations for developing the CPUF approach. For applications in low temperature kinetics, uniform conditions of temperature and pressure are required for the duration of the reaction time. The quasi-uniform flow we have discussed to this point is not suitable, as the thermodynamic parameters are constant only for 30–40 μs within the nozzle. For detection by VUV photoionization, skimmers and airfoil sampling of the uniform flow have been used to achieve sufficiently low densities in the probed region.^{26,54} We adopted a similar strategy and showed sampling could be used with mmWave detection.⁵⁵ Unfortunately, such sampling may interfere with the measurement, owing to the presence of shocks before the sampling aperture or after. Therefore, we recently developed an extended Laval nozzle, an alternative approach wherein a uniform flow is created within the nozzle itself, after which it undergoes a shock free low density secondary expansion. This is analogous to the quasi-uniform flow discussed above, except that the nozzle is long enough to ensure uniform conditions and an adequate hydrodynamic time persist inside it in which to perform kinetics. The profile of the extension is calculated to compensate for the evolution of the boundary layer thickness, which allows for the formation of a uniform flow within the tube itself. Then, the shock-free secondary expansion originating from the output of the extended nozzle can be probed, as demonstrated in the quasi-uniform flow approach described above. This new method has first been modeled through CFD simulations; however, experimental validation of the thermodynamic conditions is required before kinetic measurements. To address this, we took advantage of another probe strategy that we had developed at the same time: resonance-enhanced multiphoton ionization (REMPI) of species within the flow. By seeding a trace of NO in the flow, we could monitor the electron current on a wire anode as we scanned a probe laser across the rotationally resolved (0–

0) band of the NO A-X transition around 44200 cm^{-1} . The rotational distribution could be fitted to give the rotational temperature in the flow. To adapt this same approach to determine the temperature inside the nozzle, we produced a version of the nozzle extension in which alternating ring cathodes and anodes were embedded. The REMPI probe laser was propagated counter to the flow, and the local temperature was determined from the photoelectron yield collected at each respective anode as the laser was scanned. With this approach, we found the temperature within the flow (19.7 K) closely matched the nozzle design (20 K) and the fluid dynamics simulations (21.7 K) (Figure 7).

To demonstrate use of the extended nozzle configuration for kinetics, we chose the $\text{HCO} + \text{O}_2 \rightarrow \text{CO} + \text{HO}_2$ reaction, the first such measurement below room temperature. The experiments were carried out in pseudo-first order with respect to HCO. Furan was used as the precursor for HCO, which dissociates at 193 nm to give $\text{HCO} + \text{C}_3\text{H}_3$ as a major pathway, although other product channels are present as well.⁵⁶ The HCO reactant decay was probed on the $1_{01}-0_{00}$ ($3/2 \leftarrow 1/2$) transition at 86670.76 GHz. Figure 8(a) shows a sample kinetics trace at a single O_2 density with the window region highlighted that is used to determine the pseudo first order rate. Figure 8(b) shows the results of many such measurements plotted against the O_2 density. The slope of the plot is the bimolecular rate of the reaction, which was found to be $6.66 \pm 0.43 \times 10^{-11}\text{ cm}^3\text{ molec}^{-1}\text{ s}^{-1}$, roughly 12 times

faster than the room temperature rate. Hsu et al. examined the direct and indirect pathways contributing to the reaction and their rates in detail at the G2M(RCC)//B3LYP/6-311G(d,p) level of theory with variational treatment of the barrierless pathway and RRKM calculations.⁵⁷ They found at low temperature the reaction proceeds by formation of the long-lived intermediate HC(O)OO , which is 36.1 kcal/mol below the reactant entrance channel, which then decomposes via a loose 4-center transition state 12.6 kcal/mol below reactants to give $\text{HO}_2 + \text{CO}$.

6. CONCLUSIONS AND OUTLOOK

Although we have demonstrated some of the capabilities of the CPUF combination of a low temperature flow environment with CP-FTmmW spectroscopy, the technique is still in its infancy and has room to grow immensely in the breadth of applications. As the associated electronics continue to improve, significant advances in the sensitivity and throughput are on the immediate horizon. The capability of the approach to give absolute densities for reactants and products has not been fully exploited, but we are making use of this now in ongoing experiments. This will be a boon to future studies and is simply not feasible for LIF or REMPI-based detection. Future studies can couple laser excitation in double-resonance studies to enhance sensitivity and explore the vibrational or conformational dependence of reactivity. Vibrational distributions are both a blessing and a curse here: CP-FTmmW can be used to detect and quantify reactant vibrational satellites and explore the dependence on reactivity on vibration in direct ways.²⁹ However, the presence of considerable vibrational excitation in products dilutes the signal into many quantum states that may not cool efficiently in the flow, preventing detection or distorting inferred branching. Studies of vibrational relaxation in the flow or of the K -dependent relaxation or reaction rates are also untapped capabilities. These are exciting times for CP-FTmmW and CPUF.

AUTHOR INFORMATION

Corresponding Author

Arthur G. Suits – Department of Chemistry, University of Missouri, Columbia, Missouri 65211, United States; orcid.org/0000-0001-5405-8361; Email: suitsa@missouri.edu

Authors

Nureshan Dias – Chemical Sciences Division, Lawrence Berkeley National Laboratory, Berkeley, California 94720, United States; orcid.org/0000-0002-4518-0901
 Nicolas Suas-David – Univ Rennes, CNRS, Institut de Physique de Rennes - UMR 6251, F-35000 Rennes, France
 Shameemah Thawoos – Department of Chemistry, University of Missouri, Columbia, Missouri 65211, United States

Complete contact information is available at:

<https://pubs.acs.org/10.1021/acs.accounts.4c00489>

Author Contributions

CRedit: Nureshan Dias writing - original draft; Nicolas Suas-David writing - review & editing; Shameemah Thawoos writing - review & editing; Arthur G. Suits - writing - original draft.

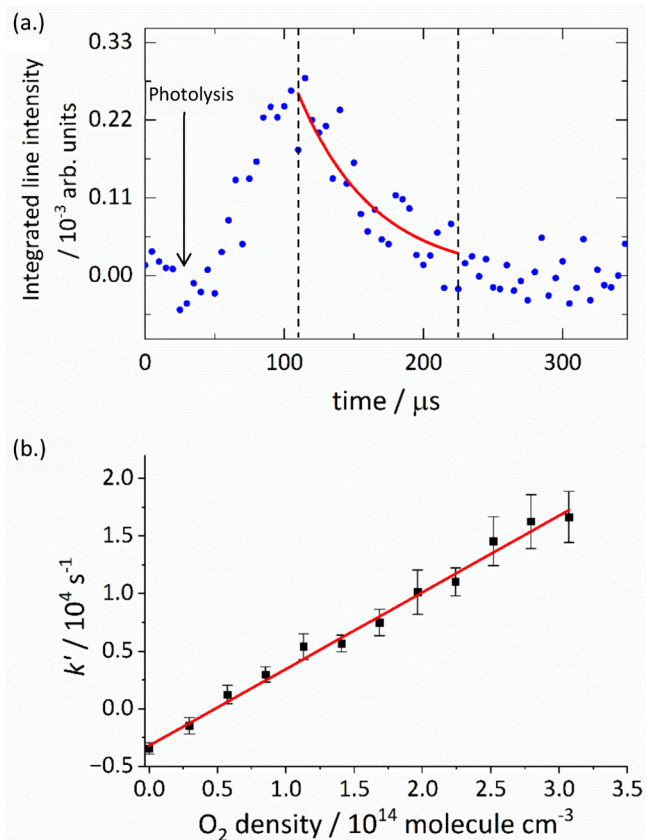


Figure 8. (a) Sample time-dependent integrated line intensities of the HCO $1_{01}-0_{00}$ line (blue filled circles) with coreactant O_2 density of $2.68 \times 10^{14}\text{ molecules cm}^{-3}$. Red solid line is the exponential fit, and the time window used for the fit is shown by two vertical dashed lines. (b) Pseudo-first-order rate constant (k') vs varying density of O_2 .

Notes

The authors declare no competing financial interest.

Biographies

Nureshan Dias was born in Kalutara, Sri Lanka, and attended the Institute of Chemistry, College of Chemical Sciences in Sri Lanka for his undergraduate studies. He earned his Ph.D. in Experimental Physical Chemistry, focusing on applications of astrochemistry and reaction dynamics, under the guidance of Prof. Arthur Suits at the University of Missouri in 2022. Following his doctoral studies, he began postdoctoral research with Musahid Ahmed at Lawrence Berkeley National Laboratory, where he is currently probing gas- and condensed-phase molecular dynamics using a range of spectroscopies.

Nicolas Suas-David was born in France and received his Ph.D. in Physics from the University of Rennes (R. Georges) in 2016. As a postdoctoral fellow, he worked at the University of Missouri-Columbia (A.G. Suits) and the Leiden Observatory (H. Linnartz) and is currently back in his first lab. His research focuses on IR spectroscopy of radicals/reaction intermediates and complex molecules (C_{60}) for astrochemistry, plasma, and combustion studies. He also designs/characterizes supersonic/hypersonic nozzles (extended Laval nozzle/Aerospike) for applications in laboratory astrophysics (spectroscopy and reaction kinetics) and space propulsion.

Shameemah Thawoos was born in Sri Lanka and completed her undergraduate studies at the University of Peradeniya. She obtained her Ph.D. in experimental physical chemistry from Prof. Arthur G. Suits at the University of Missouri and is currently Assistant Professor of Chemistry at the University of Olivet, Olivet, MI. Her interest involves studying the reaction kinetics and dynamics of astrochemically relevant reactions using the CRESU method coupled with near-IR cw-cavity ringdown spectroscopy and chirped-pulse Fourier-transformed mm-wave spectroscopic methods.

Arthur G. Suits is the Curators' Distinguished Professor of Chemistry at the University of Missouri-Columbia. Following undergraduate work at the University of Missouri, he obtained his Ph.D. from Yuan T. Lee at UC Berkeley in 1991, served as a Postdoctoral Fellow at Cornell with Paul Houston, and then took a staff position at Lawrence Berkeley National Laboratory. He has since held academic appointments at Stony Brook University and Wayne State University prior to returning to Missouri in 2016. His interests are in fundamental studies of chemical reaction dynamics and in the development of new instruments with which to pursue these studies.

ACKNOWLEDGMENTS

This work was supported by the NSF under award CHE-2247776 and by the U.S. Department of Energy (DOE) under award number DE-SC0017130.

REFERENCES

(1) Oldham, J. M.; Abeysekera, C.; Joalland, B.; Zack, L. N.; Prozument, K.; Sims, I. R.; Park, G. B.; Field, R. W.; Suits, A. G. A Chirped-Pulse Fourier-Transform Microwave/Pulsed Uniform Flow Spectrometer. I. The Low-Temperature Flow System. *J. Chem. Phys.* **2014**, *141* (15), 154202.

(2) Broderick, B. M.; Suas-David, N.; Dias, N.; Suits, A. G. Isomer-Specific Detection in the UV Photodissociation of the Propargyl Radical by Chirped-Pulse mm-Wave Spectroscopy in a Pulsed Quasi-Uniform Flow. *Phys. Chem. Chem. Phys.* **2018**, *20* (8), 5517–5529.

(3) Dias, N.; Gurusinghe, R. M.; Suits, A. G. Multichannel Radical–Radical Reaction Dynamics of NO + Propargyl Probed by Broadband Rotational Spectroscopy. *J. Phys. Chem. A* **2022**, *126* (32), 5354–5362.

(4) Thawoos, S.; Suas-David, N.; Gurusinghe, R. M.; Edlin, M.; Behzadfar, A.; Lang, J.; Suits, A. G. Low Temperature Reaction Kinetics inside an Extended Laval Nozzle: REMPI Characterization and Detection by Broadband Rotational Spectroscopy. *J. Chem. Phys.* **2023**, *159* (21), 214201.

(5) McGuire, B. A. 2021 Census of Interstellar, Circumstellar, Extragalactic, Protoplanetary Disk, and Exoplanetary Molecules. *Astrophys. J. Supp. Ser.* **2022**, *259* (2), 30.

(6) Smith, I. W.; Rowe, B. R. Reaction Kinetics at Very Low Temperatures: Laboratory Studies and Interstellar Chemistry. *Acc. Chem. Res.* **2000**, *33* (5), 261–268.

(7) Rowe, B.; Dupeyrat, G.; Marquette, J.; Smith, D.; Adams, N.; Ferguson, E. The Reaction $O_2 + CH_4 \rightarrow CH_3O_2 + H$ Studied from 20 to 560 K in a Supersonic Jet and in a SIFT. *J. Chem. Phys.* **1984**, *80* (1), 241–245.

(8) Bertelotte, C.; Lara, M.; Bergeat, A.; Le Picard, S. D.; Dayou, F.; Hickson, K. M.; Canosa, A.; Naulin, C.; Launay, J.-M.; Sims, I. R. Kinetics and Dynamics of the $S(1D_2) + H_2 \rightarrow SH + H$ Reaction at Very Low Temperatures and Collision Energies. *Phys. Rev. Lett.* **2010**, *105* (20), 203201.

(9) Sims, I.; Queffelec, J. L.; Defrance, A.; Rebrion-Rowe, C.; Travers, D.; Bocherel, P.; Rowe, B.; Smith, I. W. Ultralow Temperature Kinetics of Neutral–Neutral Reactions. The Technique and Results for the Reactions $CN + O_2$ down to 13 K and $CN + NH_3$ down to 25 K. *J. Chem. Phys.* **1994**, *100* (6), 4229–4241.

(10) Sims, I.; Smith, I.; Clary, D.; Bocherel, P.; Rowe, B. Ultra-Low Temperature Kinetics of Neutral–Neutral Reactions: New Experimental and Theoretical Results for $OH + HBr$ between 295 and 23 K. *J. Chem. Phys.* **1994**, *101* (2), 1748–1751.

(11) Potapov, A.; Canosa, A.; Jiménez, E.; Rowe, B. Uniform Supersonic Chemical Reactors: 30 Years of Astrochemical History and Future Challenges. *Angew. Chem. Int. Ed.* **2017**, *56* (30), 8618–8640.

(12) Sims, I. R.; Smith, I. W. Pulsed Laser Photolysis–Laser-Induced Fluorescence Measurements on the Kinetics of $CN(\nu=0)$ and $CN(\nu=1)$ with O_2 , NH_3 and NO between 294 and 761 K. *Journal of the Chemical Society, Faraday Transactions 2: Molecular and Chemical Physics* **1988**, *84* (5), 527–539.

(13) Sims, I. R.; Smith, I. W. Rate Constants for the Radical–Radical Reaction between CN and O_2 at Temperatures down to 99 K. *Chem. Phys. Lett.* **1988**, *151* (6), 481–484.

(14) Sims, I. R.; Smith, I. W. Rate Constants for the Reactions $CN(\nu=0)$, $CN(\nu=1) + H_2$, $D_2 \rightarrow HCN$, $DCN + H$, D between 295 and 768 K, and Comparisons with Transition State Theory Calculations. *Chem. Phys. Lett.* **1988**, *149* (5–6), 565–571.

(15) Sims, I. R.; Smith, I. W. Kinetics of $Cn(\nu=0)$ and $Cn(\nu=1)$ with HCl , HBr and HI between 295 and 764 K. *Journal of the Chemical Society, Faraday Transactions 2: Molecular and Chemical Physics* **1989**, *85* (7), 915–923.

(16) Sharkey, P.; Sims, I. R.; Smith, I. W.; Bocherel, P.; Rowe, B. R. Pressure and Temperature Dependence of the Rate Constants for the Association Reaction of OH Radicals with NO between 301 and 23 K. *J. Chem. Soc. Far. Trans.* **1994**, *90* (24), 3609–3616.

(17) Atkinson, D. B.; Jaramillo, V. I.; Smith, M. A. Low-Temperature Kinetic Behavior of the Bimolecular Reaction $OH + HBr$ (76–242 K). *J. Phys. Chem. A* **1997**, *101* (18), 3356–3359.

(18) Vakhtin, A. B.; Lee, S.; Heard, D. E.; Smith, I. W. M.; Leone, S. R. Low-Temperature Kinetics of Reactions of the OH Radical with Propene and 1-Butene Studied by a Pulsed Laval Nozzle Apparatus Combined with Laser-Induced Fluorescence. *J. Phys. Chem. A* **2001**, *105* (33), 7889–7895.

(19) Vakhtin, A. B.; Heard, D. E.; Smith, I. W.; Leone, S. R. Kinetics of C_2H Radical Reactions with Ethene, Propene and 1-Butene Measured in a Pulsed Laval Nozzle Apparatus at $T = 103$ and 296 K. *Chem. Phys. Lett.* **2001**, *348* (1–2), 21–26.

(20) Bocherel, P.; Herbert, L. B.; Rowe, B. R.; Sims, I. R.; Smith, I. W.; Travers, D. Ultralow-Temperature Kinetics of $Ch(X_2II)$ Reactions: Rate Coefficients for Reactions with O_2 and NO ($T =$

- 13–708 K), and with NH_3 ($T = 23\text{--}295$ K). *J. Phys. Chem.* **1996**, *100* (8), 3063–3069.
- (21) Brownsword, R. A.; Canosa, A.; Rowe, B. R.; Sims, I. R.; Smith, I. W.; Stewart, D. W.; Symonds, A. C.; Travers, D. Kinetics over a Wide Range of Temperature (13–744 K): Rate Constants for the Reactions of CH ($\nu = 0$) with H_2 and D_2 and for the Removal of CH ($\nu = 1$) by H_2 and D_2 . *J. Chem. Phys.* **1997**, *106* (18), 7662–7677.
- (22) Chastaing, D.; James, P. L.; Sims, I. R.; Smith, I. W. Neutral–Neutral Reactions at the Temperatures of Interstellar Clouds Rate Coefficients for Reactions of C_2H Radicals with O_2 , C_2H_2 , C_2H_4 and C_3H_6 down to 15 K. *Farad. Disc.* **1998**, *109*, 165–181.
- (23) Chastaing, D.; Le Picard, S. D.; Sims, I. R. Direct Kinetic Measurements on Reactions of Atomic Carbon, $\text{C}(3\text{P})$, with O_2 and NO at Temperatures down to 15 K. *J. Chem. Phys.* **2000**, *112* (19), 8466–8469.
- (24) Chastaing, D.; Le Picard, S.; Sims, I.; Smith, I. Rate Coefficients for the Reactions of $\text{C}(\text{P})$ Atoms with C_2H_2 , C_2H_4 , CH_3CCH and H_2CCCH_2 at Temperatures down to 15 K. *Astron. Astrophys.* **2001**, *365* (2), 241–247.
- (25) Hoobler, R. J.; Leone, S. R. A pulsed Laval nozzle apparatus with laser ionization mass spectroscopy for direct measurements of rate coefficients at low temperatures with condensable gases. *Rev. Sci. Instrum.* **2000**, *71*, 1816–1823.
- (26) Durif, O.; Capron, M.; Messinger, J. P.; Benidar, A.; Biennier, L.; Bourgalais, J.; Canosa, A.; Courbe, J.; Garcia, G. A.; Gil, J.-F. A New Instrument for Kinetics and Branching Ratio Studies of Gas Phase Collisional Processes at Very Low Temperatures. *Rev. Sci. Instrum.* **2021**, *92* (1), No. 014102.
- (27) Brown, G. G.; Dian, B. C.; Douglass, K. O.; Geyer, S. M.; Shipman, S. T.; Pate, B. H. A Broadband Fourier Transform Microwave Spectrometer Based on Chirped Pulse Excitation. *Rev. Sci. Instrum.* **2008**, *79* (5), 053103.
- (28) Abeyssekera, C.; Zack, L. N.; Park, G. B.; Joalland, B.; Oldham, J. M.; Prozument, K.; Ariyasingha, N. M.; Sims, I. R.; Field, R. W.; Suits, A. G. A Chirped-Pulse Fourier-Transform Microwave/Pulsed Uniform Flow Spectrometer. II. Performance and Applications for Reaction Dynamics. *J. Chem. Phys.* **2014**, *141* (21), 214203.
- (29) Guillaume, T.; Hays, B. M.; Gupta, D.; Cooke, I. R.; Abdalkader Khedaoui, O.; Hearne, T. S.; Drissi, M.; Sims, I. R. Product-Specific Reaction Kinetics in Continuous Uniform Supersonic Flows Probed by Chirped-Pulse Microwave Spectroscopy. *J. Chem. Phys.* **2024**, *160* (20), 204201.
- (30) Hays, B. M.; Gupta, D.; Guillaume, T.; Abdalkader Khedaoui, O.; Cooke, I. R.; Thibault, F.; Lique, F.; Sims, I. R. Collisional Excitation of HNC by He Found to be Stronger Than for Structural Isomer HCN in Experiments at the Low Temperatures of Interstellar Space. *Nat. Chem.* **2022**, *14* (7), 811–815.
- (31) Dias, N.; Gurusinghe, R. M.; Broderick, B. M.; Millar, T. J.; Suits, A. G. Direct D-Atom Incorporation in Radicals: An Overlooked Pathway for Deuterium Fractionation. *Astrophys. J.* **2023**, *944* (1), 77.
- (32) Dias, N.; Joalland, B.; Ariyasingha, N. M.; Suits, A. G.; Broderick, B. M. Direct Versus Indirect Photodissociation of Isoxazole from Product Branching: A Chirped-Pulse Fourier Transform Mm-Wave Spectroscopy/Pulsed Uniform Flow Investigation. *J. Phys. Chem. A* **2018**, *122* (38), 7523–7531.
- (33) Atkinson, D. B.; Smith, M. A. Design and Characterization of Pulsed Uniform Supersonic Expansions for Chemical Applications. *Rev. Sci. Instrum.* **1995**, *66* (9), 4434–4446.
- (34) Hansmann, B.; Abel, B. Kinetics in Cold Laval Nozzle Expansions: From Atmospheric Chemistry to Oxidation of Biomolecules in the Gas Phase. *ChemPhysChem* **2007**, *8* (3), 343–356.
- (35) Taylor, S. E.; Goddard, A.; Blitz, M. A.; Cleary, P. A.; Heard, D. E. Pulsed Laval Nozzle Study of the Kinetics of OH with Unsaturated Hydrocarbons at Very Low Temperatures. *Phys. Chem. Chem. Phys.* **2008**, *10* (3), 422–437.
- (36) Ocaña, A. J.; Blázquez, S.; Potapov, A.; Ballesteros, B.; Canosa, A.; Antiñolo, M.; Vereecken, L.; Albaladejo, J.; Jiménez, E. Gas-Phase Reactivity of CH_3OH toward OH at Interstellar Temperatures (11.7–177.5 K): Experimental and Theoretical Study. *Phys. Chem. Chem. Phys.* **2019**, *21* (13), 6942–6957.
- (37) Abeyssekera, C.; Joalland, B.; Shi, Y.; Kamasah, A.; Oldham, J. M.; Suits, A. G. Note: A Short-Pulse High-Intensity Molecular Beam Valve Based on a Piezoelectric Stack Actuator. *Rev. Sci. Instrum.* **2014**, *85* (11), 116107.
- (38) Park, G. B.; Steeves, A. H.; Kuyanov-Prozument, K.; Neill, J. L.; Field, R. W. Design and Evaluation of a Pulsed-Jet Chirped-Pulse Millimeter-Wave Spectrometer for the 70–102 GHz Region. *J. Chem. Phys.* **2011**, *135* (2), 024202.
- (39) Miller, J. A.; Klippenstein, S. J. The Recombination of Propargyl Radicals and Other Reactions on a C_6H_6 Potential. *J. Phys. Chem. A* **2003**, *107* (39), 7783–7799.
- (40) Zhou, Z.; Yang, J.; Yuan, W.; Wang, Z.; Pan, Y.; Qi, F. Probing Combustion and Catalysis Intermediates by Synchrotron Vacuum Ultraviolet Photoionization Molecular-Beam Mass Spectrometry: Recent Progress and Future Opportunities. *Phys. Chem. Chem. Phys.* **2022**, *24* (36), 21567–21577.
- (41) Agúndez, M.; Cabezas, C.; Tercero, B.; Marcelino, N.; Gallego, J.; de Vicente, P.; Cernicharo, J. Discovery of the Propargyl Radical (CH_2CCH) in TMC-1: One of the Most Abundant Radicals Ever Found and a Key Species for Cyclization to Benzene in Cold Dark Clouds. *Astron. Astrophys.* **2021**, *647*, L10.
- (42) Lombardo, N. A.; Nixon, C. A.; Greathouse, T. K.; Bézard, B.; Jolly, A.; Vinatier, S.; Teanby, N. A.; Richter, M. J.; Irwin, P. J.; Coustenis, A. Detection of Propadiene on Titan. *Astrophys. J. Lett.* **2019**, *881* (2), L33.
- (43) Klippenstein, S. J.; Miller, J. A.; Jasper, A. W. Kinetics of Propargyl Radical Dissociation. *J. Phys. Chem. A* **2015**, *119* (28), 7780–7791.
- (44) Nguyen, T. L.; Mebel, A. M.; Lin, S. H.; Kaiser, R. I. Product Branching Ratios of the $\text{C}(3\text{P}) + \text{C}_2\text{H}_3$ ($2a'$) and $\text{CH}(2\text{II}) + \text{C}_2\text{H}_2$ ($1\Sigma^+$) Reactions and Photodissociation of H_2CC^+ : $\text{CH}(2b_1)$ at 193 and 242 nm: An Ab Initio/RRKM Study. *J. Phys. Chem. A* **2001**, *105* (51), 11549–11559.
- (45) Loison, J.-C.; Agúndez, M.; Wakelam, V.; Roueff, E.; Gratier, P.; Marcelino, N.; Reyes, D. N.; Cernicharo, J.; Gerin, M. The Interstellar Chemistry of C_3H and C_3H_2 Isomers. *MNRAS* **2017**, *470* (4), 4075–4088.
- (46) Wang, X.; Song, J.; Lv, G.; Li, Z. Theoretical Study on the Reaction of Nitric Oxide with Propargyl Radical. *J. Phys. Chem. A* **2019**, *123* (5), 1015–1021.
- (47) Danilack, A. D.; Goldsmith, C. F. A Computational Investigation into the Kinetics of $\text{NO} + \text{CH}_2\text{CCH}$ and Its Effect on NO Reduction. *Proc. Combust. Inst.* **2019**, *37* (1), 687–694.
- (48) Ashfold, M. N.; King, G. A.; Murdock, D.; Nix, M. G.; Oliver, T. A.; Sage, A. G. $\pi\sigma^*$ Excited States in Molecular Photochemistry. *Phys. Chem. Chem. Phys.* **2010**, *12* (6), 1218–1238.
- (49) Cao, J. Photoinduced Reactions of Both 2-Formyl-2h-Azirine and Isoxazole: A Theoretical Study Based on Electronic Structure Calculations and Nonadiabatic Dynamics Simulations. *J. Chem. Phys.* **2015**, *142* (24), 244302.
- (50) Nunes, C. M.; Reva, I.; Pinho e Melo, T. M.; Fausto, R.; Solomek, T.; Bally, T. The Pyrolysis of Isoxazole Revisited: A New Primary Product and the Pivotal Role of the Vinylnitrene. A Low-Temperature Matrix Isolation and Computational Study. *J. Am. Chem. Soc.* **2011**, *133* (46), 18911–18923.
- (51) Geng, T.; Ehrmaier, J.; Schalk, O.; Richings, G. W.; Hansson, T.; Worth, G.; Thomas, R. D. Time-Resolved Photoelectron Spectroscopy Studies of Isoxazole and Oxazole. *J. Phys. Chem. A* **2020**, *124* (20), 3984–3992.
- (52) Lee, T. J.; Rendell, A. P. The Structure and Energetics of the $\text{HCN} \rightarrow \text{HNC}$ Transition State. *Chem. Phys. Lett.* **1991**, *177* (6), 491–497.
- (53) Koda, S.; Endo, Y.; Tsuchiya, S.; Hirota, E. Branching Ratios in Atomic Oxygen ($3p$) Reactions of Terminal Olefins Studied by Kinetic Microwave Absorption Spectroscopy. *J. Phys. Chem.* **1991**, *95* (3), 1241–1244.

(54) Soorkia, S.; Liu, C.-L.; Savee, J. D.; Ferrell, S. J.; Leone, S. R.; Wilson, K. R. Airfoil Sampling of a Pulsed Laval Beam with Tunable Vacuum Ultraviolet Synchrotron Ionization Quadrupole Mass Spectrometry: Application to Low-Temperature Kinetics and Product Detection. *Rev. Sci. Instrum.* **2011**, *82* (12), 124102.

(55) Gurusinge, R. M.; Dias, N.; Krueger, R.; Suits, A. G. Uniform Supersonic Flow Sampling for Detection by Chirped-Pulse Rotational Spectroscopy. *J. Chem. Phys.* **2022**, *156* (1), No. 014202.

(56) Sorkhabi, O.; Qi, F.; Rizvi, A. H.; Suits, A. G. Ultraviolet Photodissociation of Furan Probed by Tunable Synchrotron Radiation. *J. Chem. Phys.* **1999**, *111* (1), 100–107.

(57) Hsu, C. C.; Mebel, A.; Lin, M.-C. Ab Initio Molecular Orbital Study of the HCO + O₂ Reaction: Direct Versus Indirect Abstraction Channels. *J. Chem. Phys.* **1996**, *105* (6), 2346–2352.